NASA TN D-1

TECHNICAL NOTE

D-1

A STUDY OF THE ACOUSTIC FATIGUE CHARACTERISTICS OF SOME FLAT AND CURVED ALUMINUM PANELS EXPOSED TO RANDOM AND DISCRETE NOISE

By Robert W. Hess, Robert W. Herr, and William H. Mayes

Langley Research Center
Langley Field, Va.

NATIONAL AERONAUTICS AND SPACE ADMINISTRATION
WASHINGTON
August 1959

NATIONAL AERONAUTICS AND SPACE ADMINISTRATION

TECHNICAL NOTE D-1

A STUDY OF THE ACOUSTIC FATIGUE CHARACTERISTICS OF SOME FLAT AND CURVED ALUMINUM PANELS EXPOSED TO RANDOM AND DISCRETE NOISE

By Robert W. Hess, Robert W. Herr, and William H. Mayes

SUMMARY

A study was made of the fatigue life of simple 2024-T3 aluminum-alloy panels measuring 11 by 13 inches and exposed to both discrete-frequency noise from a siren and random noise from an air jet. Noise levels varied from approximately 140 to 161 decibels for these tests. Panel variables included thickness, edge conditions, curvature, and static-pressure differential.

No significant differences were noted in the nature of failures experienced for the two types of loadings. At a given root-mean-square stress level, the failure times were generally shorter for the random loading than for the discrete-frequency loading. These differences in failure times were noted to be a function of stress level, the larger differences occurring at the lower stress levels.

Increases in time to failure were obtained as a result of increased panel thickness, increased panel curvature, and particularly for increased static-pressure differential across curved panels.

For the discrete-type loading, the location of weak points in these simplified structural designs can be satisfactorily accomplished but quantitative predictions of fatigue life are much more difficult.

INTRODUCTION

Fatigue damage to panels and other secondary structures as a result of acoustically excited vibrations has become one of the important operating problems of high-speed aircraft. These vibrations result from the fluctuating pressure loads impinging on the aircraft surface and are due to either the noise from the power plants or the aerodynamic boundary layer or both. This problem is severe for the random noise from the

engines of jet-powered aircraft, particularly for thrust augmentation at take-off where the noise levels may exceed 160 decibels on some parts of the aircraft.

In the past, designers have relied heavily on the results of acoustic fatigue tests as a basis for improving their designs. Because it is not possible at present to predict fatigue life analytically, it appears that there is still a widespread need for this type of testing. In the interest of economy much of the testing of panel designs will be done in the laboratories as indicated in references 1 and 2. References 1 and 2 indicate that the siren, as a discrete-frequency noise generator, is very useful for evaluating the relative merits of many full-scale panel configurations by uncovering weak points in their construction.

L 1 7 6

The problem of determining the fatigue life under random acoustic loading based on results of discrete-frequency tests is a difficult one. Some information relating to this problem is given in reference 3 in which fatigue data are presented for simple flat panels exposed to both discrete and random noise. The present paper is an extension of the panel fatigue studies of reference 3. Results of additional panel tests obtained for the noise-level range from 140 to 161 decibels are included along with a more detailed discussion of the conditions of the tests and the techniques used. Comparisons are made of the fatigue life of simple panels exposed to discrete-frequency loading of a siren and random loading of an air jet. Also investigated are the effects on panel fatigue life of other variables such as noise level, panel thickness, panel curvature, static-pressure differential, and edge attachment. Supplementary information relating to panel natural frequencies and input-noise characteristics are presented in appendixes A and B.

SYMBOLS

c	disturbance velocity, ft/sec
D	panel flexural rigidity, $Eh^3/12(1 - \mu^2)$
E	Young's modulus of elasticity, psi
f	frequency, cps
Δf	band width, $f_h - f_l$
h	panel thickness, in.
l	distance between pressure cells, ft

m	mass of panel per unit area
n	number of tests
R	radius of curvature, ft
T	fatigue life of a given panel (time to first perceptible crack), min
$\overline{T}$	experimental mean fatigue life for a small number of samples, min
T_s	deviation from mean life for n tests
$\overline{T}_T$	true mean fatigue life for an infinite number of samples, min
t	time from start of test, unless otherwise noted, sec
w	panel deflection
δ	panel damping as fraction of critical damping
θ	phase angle between pressures at two points on panel, deg
μ	Poisson's ratio
$\left(\sqrt{\overline{\sigma^2}}\right)_{av}$	average root-mean-square stress for n tests
$\sqrt{\overline{\sigma^2}}$	root-mean-square stress

Subscripts:

h	high-pass cutoff frequency
l	low-pass cutoff frequency
o	natural frequency of panel
t	indicates partial derivative with respect to time
x	indicates partial derivative in x-direction
y	indicates partial derivative in y-direction

In this paper, noise level is given in decibels and is equal to $20 \log_{10}\left(\frac{p}{0.0002}\right)$ where p is pressure in dynes/cm^2.

APPARATUS AND METHODS

Test Setups

Two test setups were used in the present tests for the purpose of applying fluctuating pressure loads to the panel models. Random acoustic loads were applied with the aid of a large air jet, whereas discrete acoustic loads were applied with the aid of a conventional siren.

Random loading.- Eleven panels were tested simultaneously in the noise field of a 12-inch exit-diameter air jet operated at a high subsonic velocity. Figure 1 is a photograph of the test setup. The panels are set off from the theoretical 15° jet boundary 6 inches along the two sides and about 12 inches on the bottom. The various test stations will, hereafter, be referred to by numbers 1 to 11 which are shown in figure 1. Two additional stations will be referred to as 1' and 2', and these stations correspond to stations 1 and 2, except that the panels are located an additional 3 inches from the jet boundary.

In order to increase the noise levels at the low end of the noise spectrum at stations near the nozzle, a series of bends were put in the pipe upstream of the nozzle. Figure 2 is a photograph of this configuration. This scheme increased the noise output of the jet by 10 decibels at some of the test stations and thus made possible a wider range of input loadings for the test.

The differential acoustic pressure varied from station to station and also along the length of the panel. The overall random noise levels used in this paper represent an average differential pressure obtained from at least two cell positions distributed along the major axis of the panel. Figure 3 presents a representative pressure spectrum for stations 1', 2', and 1 to 10.

Discrete loading.- The discrete-noise generator consisted of a siren coupled to a 6-foot acoustic horn with a 2-foot exit diameter. The siren is a device in which pressurized air is fed into a stationary multihole disk over which passes another rotating multihole disk. The result is a periodic, nearly sinusoidal signal whose frequency is controlled by changing the angular speed of the rotating disk. Only one panel at a time was tested with the siren, the panel being placed approximately 6 inches from the mouth of the horn in a plane perpendicular to the horn axis.

Test Panels

Flat and curved 2024-T3 aluminum-alloy panels measuring 11 inches by 13 inches were tested. The thicknesses of the flat panels varied from 0.020 inch to 0.064 inch. Most of the tests were made with a configuration intended to simulate the stress concentrations of a riveted-edge aircraft panel mounted on a rigid supporting structure. Figure 4 is a schematic drawing of the mountings for the two basic panel configurations (flat or curved) and of the five variations in panel-edge conditions. Table I contains the types of loadings, the number of panels tested for each edge condition, and the thicknesses of the panels. Some information relating to the panel natural frequencies and the techniques used in calculating these frequencies is included in appendix A.

Random loading.- Configurations A, B, and C (fig. 4) were tested with the air jet. All panels were mounted to a 1-inch-thick aluminum plate which had a rectangular cutout $9\frac{5}{8}$ inches by $11\frac{5}{8}$ inches, corresponding to the unsupported dimensions of the panel. With the exception of configuration C which was bolted every $2\frac{1}{8}$ inches on centers, all panels were attached to the mounting plates and frames by roundhead bolts (No. 5-44) spaced $1\frac{1}{16}$ inches on centers. The bolts were tightened in a fixed sequence to a preselected constant torque on each specimen.

As may be noted in table I, most tests were made with 0.032-inch and 0.064-inch panels having an end fixity of configuration A.

In an attempt to evaluate the merits of various types of edge conditions, configurations B and C were also tested in limited number. The section view of configuration B (fig. 4) illustrates an intermediate configuration in which the panel is bonded with Epon VI to a 1/2- by 1-inch aluminum frame on the bottom surface only.

The section view of configuration C (fig. 4) shows the configuration used to obtain a bonded edge condition. In this arrangement the test panel was bonded with Epon VI to a 1/2- by 1-inch aluminum frame on both top and bottom surfaces. These variations in edge conditions were tested with 0.032-inch panels only.

Discrete loading.- Both flat- and curved-panel configurations were fatigue tested using periodic excitation. Flat panels ranging in thickness from 0.020 inch to 0.064 inch were bolted to the same aluminum plates used in the air-jet studies. The curved panels with the same dimensions as the flat panels were 0.032 inch thick and were rolled to 4-foot and 8-foot radii. These panels were mounted on a curved steel

frame of the same radius which was attached to a 1-inch aluminum plate as shown in figure 4. The curved panels consisted of configurations D and E which are also illustrated in figure 4.

The panel mounting plates were fastened to a chamber which contained filler material to minimize standing waves. The chamber was used in studying the effects of static-pressure differential on the fatigue life of curved panels. It was found that the chamber and enclosed material had little effect on the measured panel damping.

L 1 7 6

Instrumentation

Provision was made for measuring the input acoustic loading on the panels, the corresponding stress response at an arbitrary point on the panel, and the elapsed time to the first perceptible fatigue crack. In addition, provision was made for frequency analyses of the stress and acoustic pressure data for some test conditions.

Random loading.- The differential acoustic loading at each station was determined from measurements obtained with miniature electrical pressure gages (ref. 4) mounted in a rigid 1/4-inch aluminum plate. Eight gages were equally spaced, $1\frac{1}{4}$ inches between centers, along the major axis of the plate. The outputs of the eight gages were simultaneously recorded on a 14-channel FM tape recorder.

Panel stress response for all tests was determined from the output of a Baldwin SR-4 type A-8 strain gage located as shown in figure 4. The gage was located as near as possible to the center hole on one of the short sides in an effort to measure stress at the point where fatigue usually occurred. Even so, the strain gage is a little over 1-hole diameter from the edge of the hole and thus probably does not indicate the maximum stress.

The strain-gage outputs were fed through eight linear amplifiers to a bank of thermocouple meters for direct observations of the root-mean-square stress. The outputs were also recorded directly on a 14-channel FM tape recorder for analysis with a constant-band-pass analyzer.

The overall frequency response of both meter and recording systems was flat from about 5 cps to 1,000 cps, the 3-kcps carrier amplifier being the limiting component at higher frequencies. Since this range covers the first 9 or 10 natural frequencies of the 0.032-inch panels and the first 6 or 7 natural frequencies of the 0.064-inch panels, it was considered to be adequate.

The tape-recorded strain-gage data were played back into thermocouple meters to obtain root-mean-square stress for cases where meter readings were not obtained directly during the tests. In addition, some strain-gage tape records were played back into a frequency analyzer to determine the frequency content of the panel response to the random noise loading of the air jet. Tape records of the input noise pressure were played back into a constant-band-width (10 cps) correlation analyzer for determination of power spectra and cross spectra.

Discrete loading.- The noise level, time to failure, and the stress-time history were recorded for each panel tested. The signal from the strain gage was amplified by a 3-kcps carrier amplifier and recorded by a recording oscillograph (flat to 200 cps). The siren frequency was adjusted to provide a maximum panel fundamental mode stress response as indicated by the strain-gage signal displayed on a panoramic analyzer. The strain gage often failed early in the test, however, and an auxiliary method was thus necessary to assist in maintaining the proper siren frequency. An inductance pickup was centered behind the panel to sense panel deflections. Its output was amplified and then monitored visually with the aid of an oscillograph to provide an indication of relative vibration amplitude. This setup was augmented for the curved panels by the addition of a high-frequency galvanometer in the recording oscillograph and a root-mean-square meter and its attendant linear amplifier and thermocouple. The high-frequency galvanometer (flat to 600 cps) was necessary because the natural frequency of curved panels increased when the panels were subject to a static-pressure differential. The root-mean-square meter was used to obtain direct stress readings during the tests.

The reference noise level at the panel was determined with the aid of a condenser-type microphone located close to the surface supporting plate near the edge of the panel. The microphone was calibrated to indicate the noise levels that would exist at the surface of a rigid flat plate placed in the noise field in a manner similar to the test panels.

Experimental Technique

Random loading.- The tests consisted of operating the air jet at a chosen stagnation pressure for varying lengths of time and then bypassing the air supply to the test cell while the panels were being inspected for cracks with a magnifying glass. Stations 1 and 5 (fig. 1), where fatigue occurred in 1 to 10 minutes, were constantly monitored for fatigue cracks with a telescope mounted in the observation room above the test cell. This was necessary because the fatigue life at these stations was considerably shorter than the periods between shutdown. Observation with a telescope was roughly equivalent to close observation with the naked eye; the telescope also supplemented shutdown and inspection techniques for stations 2 and 6, where fatigue life occurred in 30 to 100 minutes. It is recognized that the shutdown and inspection procedure used for the

remaining stations restricts the discovery of a crack to certain intervals, but since the inspection intervals which varied from 1 minute to 30 minutes were considerably less than the mean fatigue life, the errors are believed to be small.

In order to keep the acoustic input to the panels as nearly constant as possible, two quantities were used to set the air-supply compressor. First, the jet stagnation pressure was used as a crude basis for equality from day to day. Secondly, the root-mean-square stress at station 8, where failure never occurred, was monitored. This latter quantity was used as a basis for fine adjustment of the compressor output. Ordinarily, the two monitoring systems tracked together, although an occasional cold or very humid day produced significant differences. At such times the stress at station 8 was used as the basis for compressor control.

Discrete loading.- All siren fatigue data were obtained by exciting the panels in the first natural mode. The frequency of the first mode was determined by visually monitoring the strain-gage output in the recording oscillograph and panoramic analyzers for maximum amplitude. Before the actual fatigue tests began, the panel natural frequencies were determined from shake tests. Membrane stresses stiffen the panel at large deflections. (See appendix A.) This stiffening manifests itself in an increase in panel natural frequency with increasing noise level. Therefore, the usual test procedure was to determine the first-mode frequency at a low noise level. The air-supply pressure was then increased and the siren frequency was continuously adjusted to maximum strain-gage response until the desired noise level was obtained.

The first few panels of a test sequence gave a rough approximation of the fatigue life, and as succeeding panels approached this fatigue life the frequency of inspections was increased. The rate of increase of localized change in surface texture of the panel between inspections was also used as an indication of impending fatigue. This inspection procedure made it possible to determine the fatigue life of a panel to within a small fraction of the total life for panels with a fatigue life over 3 or 4 minutes. However, as the noise levels are increased and the panel fatigue life decreases, an increasingly larger portion of the fatigue life is spent adjusting the siren to the proper revolutions per minute and noise level, and the fatigue life of a panel at a given noise level becomes less certain.

The testing procedure used with curved panels varied from that used with flat panels only when the curved panel was pressurized. In this case, the mounting chamber and the concave surface of the panel were pressurized to either 5 or 13 inches of mercury and the pressure in the chamber was kept at a constant level by continuously monitoring.

STATISTICAL QUANTITIES USED IN EVALUATING DATA

Since certain statistical quantities are helpful in handling the accumulated fatigue data, these quantities are briefly discussed.

Consider the case where there are n values of the quantity T, that is, T_i (where $i = 1, 2, 3, \ldots n$) at essentially constant stress. The mean fatigue life $\overline{T}$ is defined as

$$\overline{T} = \sum_{i=1}^{n} \frac{T_i}{n}$$

This value of $\overline{T}$ is the average of the measured values and in general will not be equal to $\overline{T}_T$ the true mean fatigue life of an infinite number of tests. Statistical theory, however, provides techniques which permit the determination of the range or interval within which the true value will lie for given levels of probability. Such intervals are termed confidence intervals or limits. The procedure (ref. 5) provided for determining these intervals is so constructed that the intervals selected will enclose the true mean fatigue life $\overline{T}_T$ with a given probability, for instance 95 percent. As indicated in reference 5, the 95-percent confidence limits for the mean values are given by

$$\overline{T} - t_{.05} \frac{T_s}{n - 1} < \overline{T}_T < \overline{T} + t_{.05} \frac{T_s}{n - 1}$$

where T_s is the standard deviation defined by

$$T_s = \sqrt{\frac{\sum_{i=1}^{n} (T_i - \overline{T})^2}{n}}$$

and $t_{.05}$ designates a value appropriate for the 95-percent confidence limit and is obtained from tables of the student's t distribution (table IV, ref. 5). The value $t_{.05}$ depends on the number of observations and decreases with increasing n.

RESULTS AND DISCUSSION

The results are separated into two categories: the effects of various panel parameters on fatigue life and a comparison of fatigue life of similar panels subjected to random and discrete inputs. The parameters considered are: end condition, thickness, curvature, and static-pressure differential on a curved panel. A comparison of fatigue life for the two types of loadings is made on a noise-level basis and on a stress basis.

L 1 7 6

Effects of Various Panel Parameters on Fatigue Life

Flat-panel edge condition.- Station 1' of the air jet was used to test three families of 0.032-inch flat panels employing configurations A, B, and C (fig. 4). The results represent a direct comparison of fatigue life in terms of time to failure for the three configurations. These different configurations experienced the same input loading, since the natural frequencies of the panels varied only slightly with edge conditions. Figure 5 gives a comparison of the fatigue life of these three configurations. Due to the scatter of the data, the experimental mean fatigue life $\overline{T}$ does not give a reliable gage of the relative merits of the configurations. It will be noted that the 95-percent confidence intervals for the single-bonded panels overlap those of both the bolted and the double-bonded panels, and the only conclusion which can be reached is that this configuration is at least as good as the bolted panel. Only in the comparison of the bolted and double-bonded panels is a conclusion of definite superiority warranted.

An interesting sidelight of these tests is the manner in which the damage progresses after the development of a crack. As discussed in reference 6, the cracks, which start at stress concentrations near the bolt heads, grow until a union of the cracks occurs between bolt heads. Ultimately, a crack results which runs the full length of the side, as shown in figure 6. This usually takes a significant length of time, perhaps half of the time to initial failure. With the single-bonded panels, the failures followed the same pattern after the bond failed. With the double-bonded panels, however, the earliest detection of a crack usually occurred only after it ran perhaps half the length of a side and in many cases the first indication of fatigue occurred only when the entire side had cracked completely. In many instances the entire side failed between inspection (telescope) periods which were approximately 1 minute. Thus, on the basis of these tests, it appears that the double-bonded panel no longer has any significant advantage over the bolted panel if complete failure of a panel were the fatigue criterion.

Panel thickness.- The effects of panel thickness on time to failure were studied with both the air jet and the siren. Figure 7 presents

air-jet data taken at stations 1, 1', and 5 for flat-bolted 0.032-inch and 0.064-inch panels. The 0.064-inch panels did not always develop fatigue cracks near the bolt head. The first detectable crack usually occurred where the panel bends over the cutout edge in the mounting plate. When the 95-percent confidence limits are used, the 0.064-inch panel has a fatigue life that is about 12 times longer than the 0.032-inch panel at station 1 and about 11 times longer at station 5. No conclusions can be drawn at station 1' because of the lack of sufficient fatigue data for the 0.064-inch panel.

Figure 8 gives results of fatigue tests of 0.020-inch and 0.040-inch panels as well as for 0.032-inch and 0.064-inch panels vibrating in the first mode at a discrete noise level of 150 decibels. The data for the 0.020-inch panel are not to be considered as reliable as the data for the other three panels because of the short fatigue life at this noise level and also because severe buckling occurred before the testing conditions were stabilized. On the basis of the 95-percent confidence limits, only the 0.064-inch panel shows any substantial increase in fatigue life due to thickness. Part of this increase in fatigue life is due to the manner in which the 0.064-inch panel failed, in that it cracked near the plate cutout edge rather than near the bolt head. There is no increase in life due to thickness for the other three panels at this high noise level.

For the discrete frequency tests, it is interesting to note that the minimum ratio of the fatigue life for the 0.064-inch panel to the fatigue life for the 0.032-inch panel is about 15, based on the 95-percent confidence limits. This ratio is of the same order of magnitude as that corresponding to the 0.064-inch and 0.032-inch panels subjected to the random loading of the air jet. This latter result and the fact that the types of failures were similar in both cases suggest the feasibility of using the more economical siren for testing the relative merits of various simple configurations, such as those of these tests.

Curvature.- The effects of curvature on the fatigue of panels vibrating in the first mode were investigated for three different radii of curvature at a discrete noise level of 154 decibels. The results of these tests are presented in figure 9 where time to failure is plotted against $1/R$ for $R = \infty$, 8 feet, and 4 feet. The most significant increase in fatigue life is the increase of radius from the flat panels to the panel with a radius of curvature of 8 feet. Not all of the increase in fatigue life is due to the stiffening effects of curvature. Part of the increase in fatigue life is due to the different nature of the failure for the flat panels and the curved panels. The flat panels (configuration A) failed near the bolt heads whereas the curved panels (configuration D) generally failed on the long edge of the panel near the edge of the supporting frame.

Static pressure.- The benefits of the static-pressure differential on the first-mode fatigue life of a 0.032-inch panel with a radius of curvature of 8 feet is indicated in figure 10. Fatigue life is plotted as a function of static-pressure differential for a discrete noise level of 154 decibels. The panels were fatigued with a static gage pressure (positive pressure in the chamber) of 0 psi, 2.25 psi, and 6.37 psi. A positive pressure in the chamber exerted a sufficient force to lift the panel off the edge of the supporting frame (configuration D) so that the fatigue of the pressurized panels occurred not at the frame edge but at a stress concentration at the bolt holes. In this test the radius-edge frame (configuration E) was used for the unpressurized panels so that fatigue occurred near the bolt head for all conditions. When the 95-percent confidence limits were used, the panel with a static-pressure differential of 2.25 psi has a fatigue life which is at least twice as long as the unpressurized panel. The confidence limits of the panels with a static-pressure differential of 6.37 psi overlap the confidence interval of the panels with a static-pressure differential of 2.25 psi, although there is a factor of 1.3 in their mean lives.

A comparison of the sharp-edge fatigue data of figure 9, which is replotted in figure 10, with the radius-edge fatigue data of the unpressurized panels of figure 10 makes it possible to assess the effects of the stress concentrations near the bolt head of the unpressurized 8-foot curved panels. When the 95-percent confidence limits of the two sets of data are used, the panels that failed along the supporting edge can be expected to last longer.

Comparison of Fatigue Life of Panels Subject to Both Random and Discrete Noise Inputs

A comparison of the fatigue life of 0.032-inch panels tested with the air jet and the siren is presented as a function of overall noise level in figures 11 and 12 and is presented as a function of root-mean-square stress in figure 13. The mean fatigue life and confidence interval as well as the average root-mean-square stress are given for each family of panels for the air jet and siren in tables II and III, respectively. The air jet was run at essentially a constant nozzle-pressure ratio so that variation in noise level and fatigue life is a function of panel position with regard to the nozzle. Accordingly, the air-jet fatigue data are coded by stations.

Effect of overall noise level.- The plot of fatigue life as a function of overall noise level, figure 11, illustrates the inherent differences in the results for the two types of noise inputs. Curves are faired through the mean values of each family of data points for the air-jet and siren data. It should be noted that the random noise levels of figure 11 cover the band width from 0 to 1,000 cps.

The siren data fall generally to the left of the air-jet data in figure 11 and there is a tendency for the two curves to diverge at the lower noise levels. For the panels tested, the ratio of fatigue lives of the air-jet tests to the fatigue lives of the siren tests is approximately 6 to 1 at a noise level of 158 decibels and may approach infinity at noise levels less than 146 decibels. These differences in fatigue life may result partially from the fact that all of the noise from the siren is purposely concentrated at the first natural frequency of the panel, whereas a relatively small percentage of the impinging air-jet noise corresponds in frequency to the panel natural frequencies and thus is accepted by the panel.

Both sets of data exhibit the large amount of scatter that is characteristic of fatigue data. In particular, it is noted that the data from jet stations 1' and 2' fall somewhat out of line with data from other stations. This scatter of the data from different stations may be partially explained by the differences in the noise correlation functions from one station to another, as discussed in appendix B, and also by the differences in the noise spectra.

In order to account for some of these differences in the spectra, the data of figure 11 are analyzed for two additional band widths and are presented in figure 12 along with the faired curves of figure 11. The bottom curve of figure 12 was constructed from the original air-jet data by reducing it to a unit band width. It can be noted that the data for stations 1' and 2' are well within the scatter range of the tests and appear to be consistent with data for the other stations.

Data were also analyzed for an estimated band width ($\Delta f = 2\delta f_o$) centered at the panel first natural frequency f_o. Analysis of the panel stress-response records indicated that the panels responded to random noise primarily in the first natural mode. The damping δ as a function of root-mean-square stress was obtained from figure 10 of reference 6. The average value of root-mean-square stress for each station was obtained from table II.

It is significant to note that the siren noise level required to produce failure at a given time is greater than the random noise level for a band width equivalent to the panel band width.

Effect of root-mean-square stress.- A comparison of the time to failure as a function of root-mean-square stress is presented in figure 13 for the two types of noise inputs. The flagged air-jet points designate fatigue points where the strain gage failed before a stress reading could be obtained and are plotted at the average root-mean-square stress for each station. The faired curves of figure 13 were determined with the aid of the method of least squares where the assumed curve was a straight

line on the log-log plot. The short-dashed portion of each curve indicates where the method of least squares is not believed to be applicable.

In this case, the siren curve falls to the right of the air-jet curve and there is a tendency for the two curves to converge at the higher stress levels. It is believed that this result is attributable to the difference in the stress response of the panel to these different loadings. For a given root-mean-square stress, the individual peaks are at a constant level for the siren, whereas a panel tested with the air jet responds in an irregular manner such that some individual stress peaks are above the mean stress level and some are below. The tendency for the two curves to diverge at low stress levels may be due to the fact that the peak-stress excursions have the most significant effects at the lower noise levels.

From figure 13 it can be seen that the relative times to failure for the random and discrete loadings of these tests varied according to the panel stress level. Thus, considerable caution should be exercised in the use of siren tests as a basis for predicting the time to failure in a random-noise field.

CONCLUSIONS

The results of acoustic fatigue tests using random and discrete-frequency loading on the simplified panels described herein indicate the following conclusions:

1. Increases in time to failure were obtained as a result of increased panel thickness, increased panel curvature, and particularly for increased static-pressure differential across curved panels.

2. The structural failures produced were similar in nature for both the discrete- and random-loading tests.

3. At a given root-mean-square stress the times to failure were generally shorter for the random loading than for the discrete frequency loading. These differences in failure times were noted to be a function of stress level, the larger differences occurring at the lower stress levels.

4. With regard to the role of discrete-frequency testing in these simplified structural designs, it follows that the location of weak points

in the design can be satisfactorily accomplished but quantitative predictions of fatigue life are much more difficult.

Langley Research Center,
National Aeronautics and Space Administration,
Langley Field, Va., January 7, 1959.

APPENDIX A

PANEL NATURAL FREQUENCIES

Since the identification of predominant vibration modes of a panel subject to random loading may be useful in modifications designed to prevent fatigue failure, it is desirable to be able to calculate the natural frequencies of the panel. An approximation of the panel natural frequencies has also been found useful in calculating stress (ref. 6) and in the designing of experimental panels to the full advantage of the output spectrum of existing apparatus.

The natural frequencies of a panel are directly dependent on the panel thickness as indicated by the following linear differential equation governing the transverse vibration of a flat panel:

$$w_{xxxx} + 2w_{xxyy} + w_{yyyy} = \frac{m}{D} w_{tt} \qquad (1)$$

(See ref. 7.) Two solutions of equation (1) are given in references 8 and 9.

A comparison of experimental and calculated natural frequencies at small vibration amplitudes for flat panels of various thicknesses is presented in figure 14. The experimental natural frequencies were obtained by vibrating the panels with a loudspeaker and observing the node lines. (See fig. 15.) The calculated results were obtained from equation (1) by the method outlined in reference 9. The results of figure 14 are for small deflections and would not be expected to yield good results for nonlinear deflections. As is discussed in reference 9, when deflections become large, membrane stresses become important and increase the effective stiffness of the panel, and the linear theory used in references 8 and 9 will not give accurate values of the panel frequencies. As in reference 9, for noise levels in the neighborhood of 150 decibels, experimental and calculated results are in close agreement only when the ratio of length or width to thickness is less than approximately 200.

The variation of frequency with curvature was also investigated, and the results that were obtained are in accordance with Reissner's work on the natural frequencies of curved beams (ref. 10). Figure 16 presents the experimental natural frequency of 0.032-inch curved panels with three

different radii of curvature (R = ∞, 8 ft, and 4 ft). The results indicate that there is very little difference in the natural frequencies of curved panels and flat panels when the node lines are parallel to the axis of curvature.

APPENDIX B

PRESSURE CORRELATION STUDY

As mentioned in the text, a pressure survey yielded simultaneous tape recordings of the fluctuating pressures at eight points along the center line of each panel station. The intent was to analyze these data to determine the degree to which pressures at various points on a panel were correlated. Because of the limited scope of the analysis and because of some inadequacies of the procedures used, only a rough measure of this correlation was obtained. The following paragraphs summarize the technique employed in making the correlation study and the nature of the results obtained.

The signals from two gages were transcribed on a two-channel tape, which was then formed into a loop; the time period covered by this loop was about 8 seconds. The signals from this loop were fed through separate but similar variable-frequency band-pass filters having a band width of about 10 cps; the filtered outputs were thus roughly sinusoidal with a frequency equal to the set band-pass frequency of the filters. These filtered signals were then fed into a multiplier, and the multiplied value in turn through a mean-square averaging meter, the reading of which is an indication of the co-power that exists between the original signals. To obtain the quadrature power, one of the filtered signals was first fed through a 90° phase shift unit before going on to the multiplier and then the averaging meter, which in this instance indicates the quadrature power. The phase angle that exists between the two filtered signals follows from the equation

$$\theta = \tan^{-1} \frac{\text{Quadrature power}}{\text{Co-power}}$$

Some results as obtained by this procedure follow: At station 1' for two pressure cells separated by 8.75 inches, it was found that the mean values of the phase angle θ for a frequency of 140 cycles per second was 72.8°, with variations of $\pm 3^{\circ}$. At station 3 for the same separation distance and frequency, the mean phase angle was noted to be 80°, but a variation from the angle of $\pm 45^{\circ}$ occurred. The above results suggest that the pressures were well correlated at station 1', whereas they were not well correlated at station 3. This result is further substantiated by the fact that lower stress levels and longer fatigue life were obtained at station 3 than at station 1', even though the noise levels were about the same.

If it is assumed that the pressure disturbance at a point which is moving with the flow remains essentially constant for distances traveled in the order of a panel length or less, then it may be shown that the phase angle that exists at a given frequency between the pressures at two points on the panel is given by the relation

$$\theta = 360\ f\ \frac{l}{v}$$

where f is the chosen frequency; l, the separation distance; and v, the transport or propagation velocity of the flow. On the basis of the phase angles and separation distance given in the previous paragraph, the propagation velocity for this assumed type of flow is found to be about 500 feet per second. This velocity is noted to be about one-half the maximum exit velocity of the jet and is about equal to the local velocity in the region of the jet, where the maximum turbulence levels are measured. (See ref. 12.)

REFERENCES

1. Edson, John R.: Review of Testing and Information on Sonic Fatigue. Structural Dev. Note No. 38 (Doc. No. D-17130), Boeing Airplane Co., Mar. 7, 1957.

2. Belcher, Peter M.: The High Intensity Siren as an Instrument for Fatigue Testing of Aircraft Structure. Douglas Aircraft Co., Inc. (Presented at Specialists' Meeting of Inst. Aero. Sci., Los Angeles, Feb. 26, 1957.)

3. Hess, Robert W., Fralich, Robert W., and Hubbard, Harvey H.: Studies of Structural Failure Due to Acoustic Loading. NACA TN 4050, 1957.

4. Patterson, John L.: A Miniature Electric Pressure Gage Utilizing a Stretched Flat Diaphragm. NACA TN 2659, 1952.

5. Hoel, Paul G.: Introduction to Mathematical Statistics. Second ed., John Wiley & Sons, Inc., c.1954, pp. 226, 320-321.

6. Lassiter, Leslie W., and Hess, Robert W.: Calculated and Measured Stresses in Simple Panels Subject to Intense Random Acoustic Loading Including the Near Noise Field of a Turbojet Engine. NACA Rep. 1367, 1958. (Supersedes NACA TN 4076.)

7. Webster, Arthur Gordon: Partial Differential Equations of Mathematical Physics. Second Corrected ed., Hafner Pub. Co., Inc. (New York), 1950, p. 43.

8. Warburton, G. B.: The Vibration of Rectangular Plates. Proc. Inst. Mech. Eng. (London), vol. 168, 1954, pp. 371-384.

9. Hess, Robert W.: A Method for Determining the Natural Frequencies and Mode Shapes of a Flat Panel Clamped on Four Edges. M.A.E. Thesis, Univ. of Virginia, 1956.

10. Reissner, Eric: Note on the Problem of Vibrations of Slightly Curved Bars. Jour. Appl. Mech., vol. 21, no. 2, June 1954, pp. 195-196.

11. Howes, Walton L., Callaghan, Edmund E., Coles, Willard D., and Mull, Harold R. (with Appendix B by Conger, Channing C., and Berg, Donald F.): Near Noise Field of a Jet-Engine Exhaust. NACA Rep. 1338, 1957. (Supersedes NACA TN 3763 by Howes and Mull and TN 3764 by Callaghan, Howes, and Coles.)

12. Richardson, E. G., ed.: Technical Aspects of Sound. Vol. II - Ultrasonic Range, Underwater Acoustics. Elsevier Pub. Co. (New York), 1957, pp. 360-361.

TABLE I

PANELS TESTED

Type of loading	Thickness, in.	Number of panels tested for configuration[a] -				
		A	B	C	D	E
Random	0.032	127	16	14	--	-
	.064	27	--	--	--	-
Discrete	0.020	5	--	--	--	-
	.032	45	--	--	31	4
	.040	5	--	--	--	-
	.064	8	--	--	--	-

[a]See figure 4.

TABLE II

SUMMARY OF AIR-JET FATIGUE RESULTS FOR 0.032-INCH FLAT BOLTED PANELS

Station	n	$\overline{T}$, min	$\left(\sqrt{\overline{\sigma^2}}\right)_{av}$, psi	95-percent confidence interval for $\overline{T}$	95-percent confidence interval for $\left(\sqrt{\overline{\sigma^2}}\right)_{av}$
1	16	2.23	8,862	1.80 to 2.66	8,308 to 9,416
2	14	31.84	5,202	25.61 to 38.07	4,509 to 5,895
3	15	205.50	3,844	134.25 to 276.75	3,518 to 4,170
5	18	4.05	7,851	3.24 to 4.86	7,480 to 8,222
6	21	78.89	4,420	56.83 to 100.95	4,088 to 4,752
7	5	623.00	3,685	334.6 to 991.36	3,173 to 4,197
9	12	134.10	4,335	96.81 to 171.39	3,922 to 4,748
1'	15	12.93	6,731	11.71 to 14.15	6,198 to 7,264
2'	11	144.39	3,747	106.83 to 181.95	3,188 to 4,306

TABLE III

SUMMARY OF SIREN FATIGUE RESULTS FOR 0.032-INCH FLAT BOLTED PANELS

Noise level, db	n	$\overline{T}$, min	$\left(\sqrt{\overline{\sigma^2}}\right)_{av}$, psi	95-percent confidence interval for $\overline{T}$	95-percent confidence interval for $\left(\sqrt{\overline{\sigma^2}}\right)_{av}$
157	7	0.71	(a)	0.42 to 1.00	(a)
154	8	1.17	9,320	.52 to 4.82	8,061 to 10,578
150	7	4.00	8,830	2.42 to 5.57	7,646 to 10,010
144	11	28.65	7,080	15.65 to 41.65	6,105 to 8,043
139.5	4	133.5	-----	99.6 to 467.4	----------

[a]Strain gages were destroyed before noise level was stabilized.

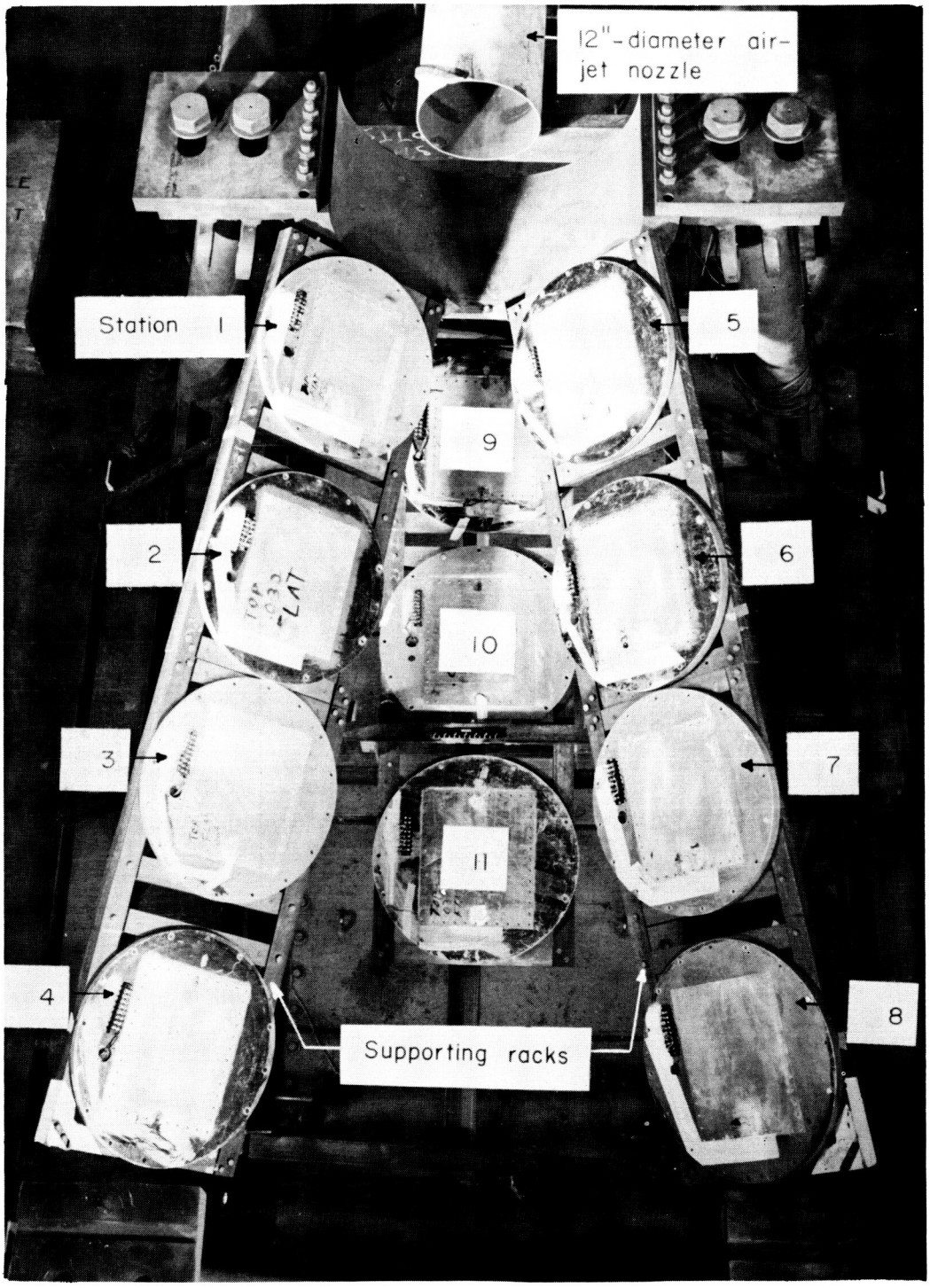

L-57-689.1

Figure 1.- Plan-view orientation of panel stations to air jet.

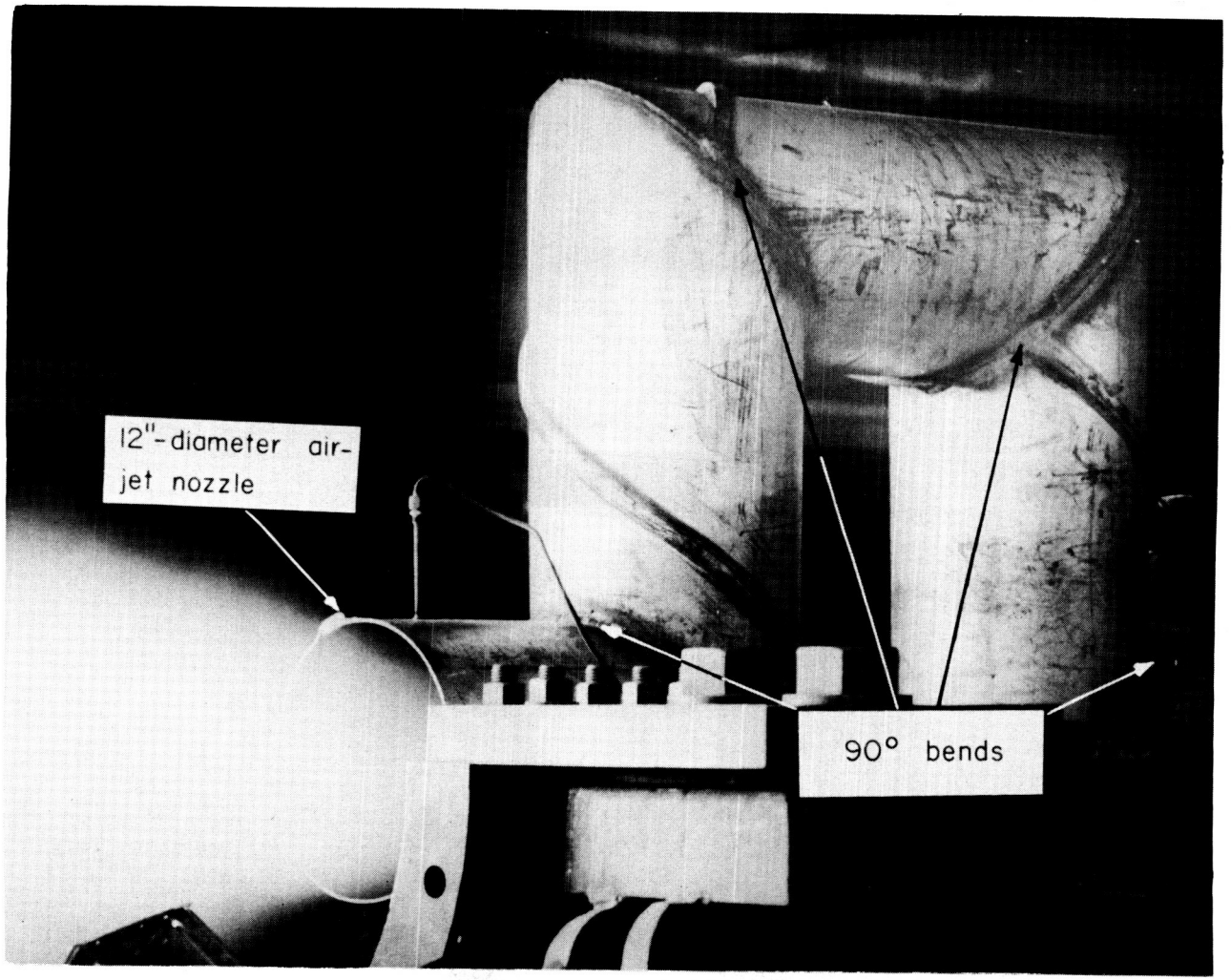

L-57-788.1

Figure 2.- Side view of air-jet test setup showing the 90° bends in the pipe upstream of the nozzle.

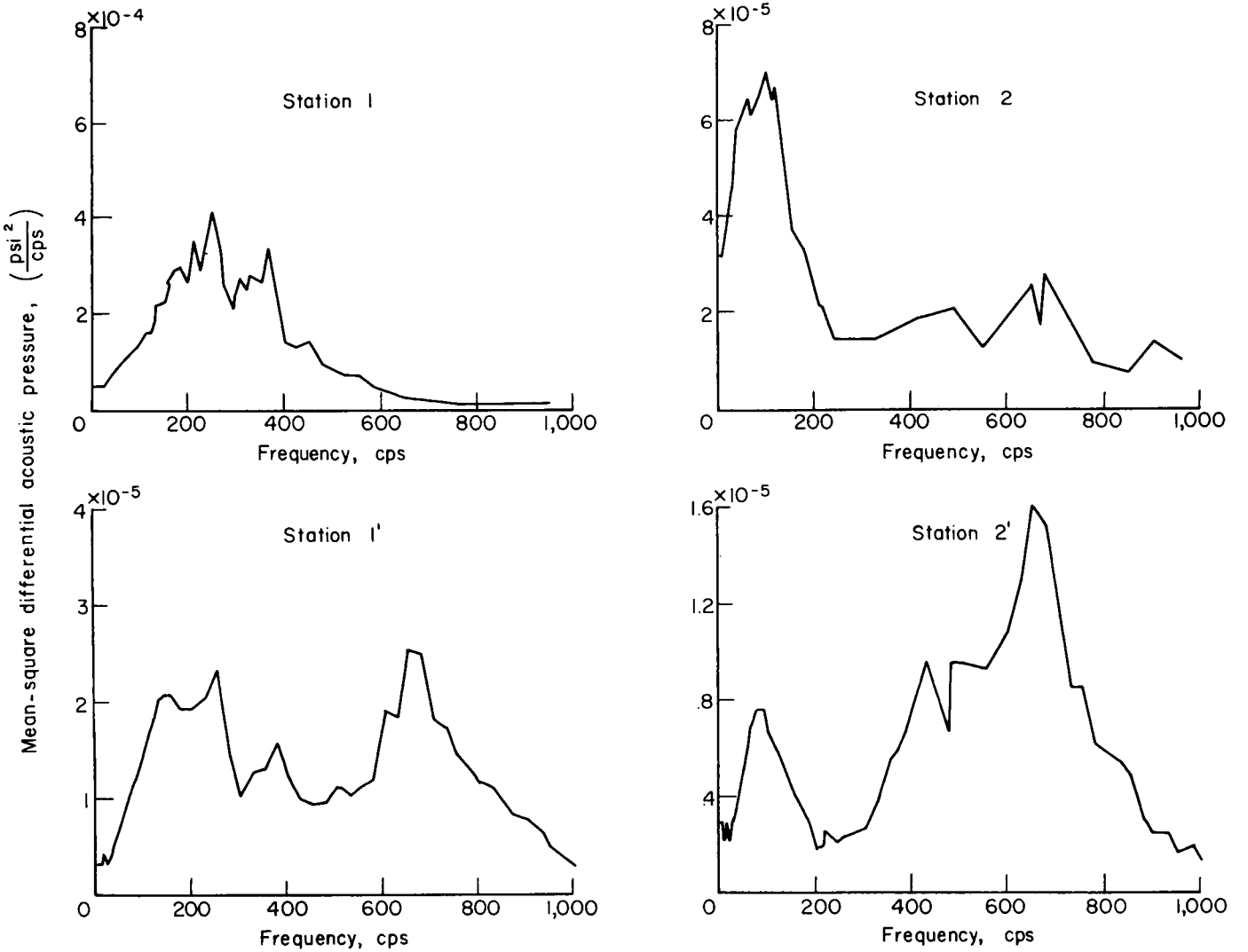

Figure 3.- Representative mean-square acoustical pressure per unit band width as a function of frequency for each air-jet test station.

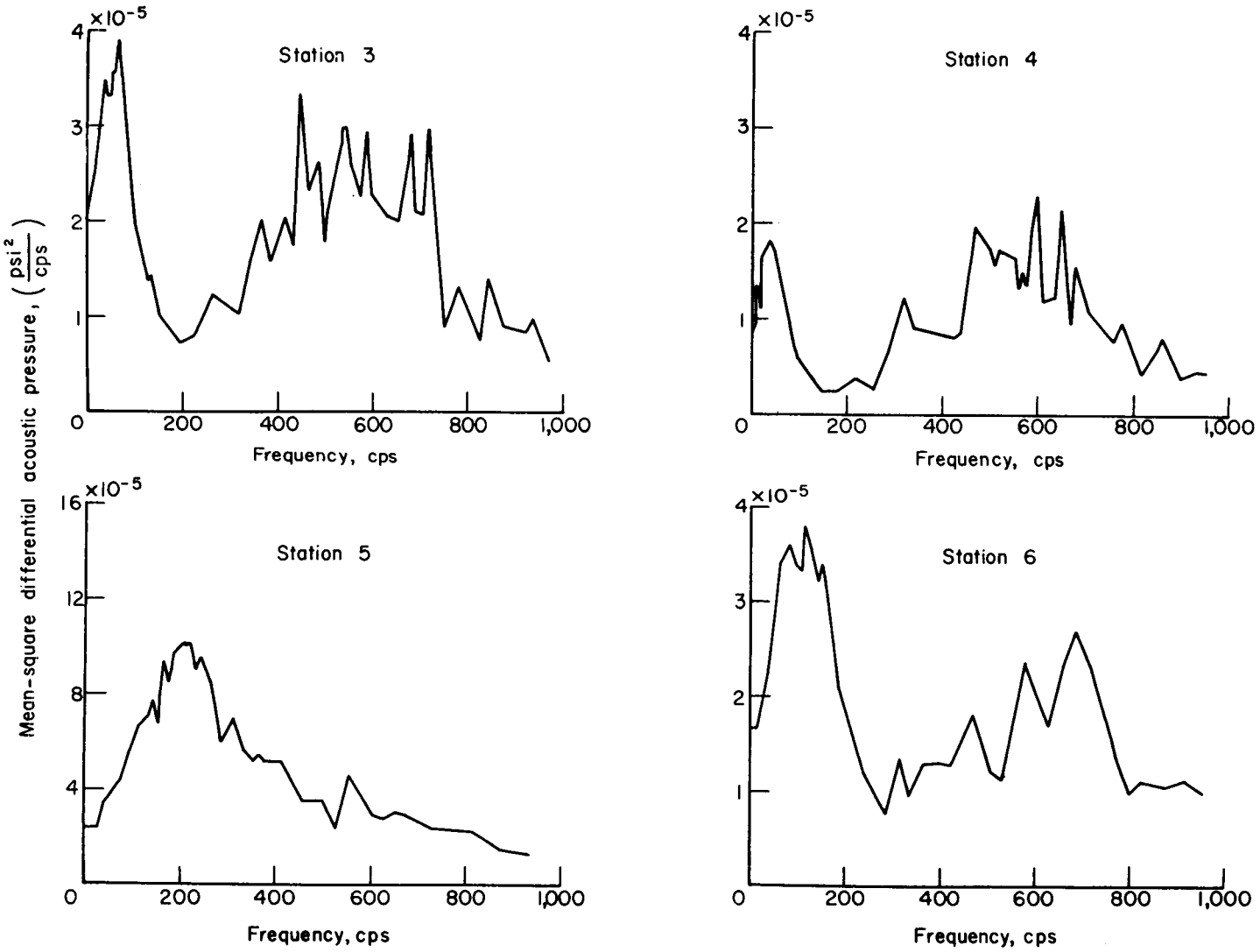

Figure 3.- Continued.

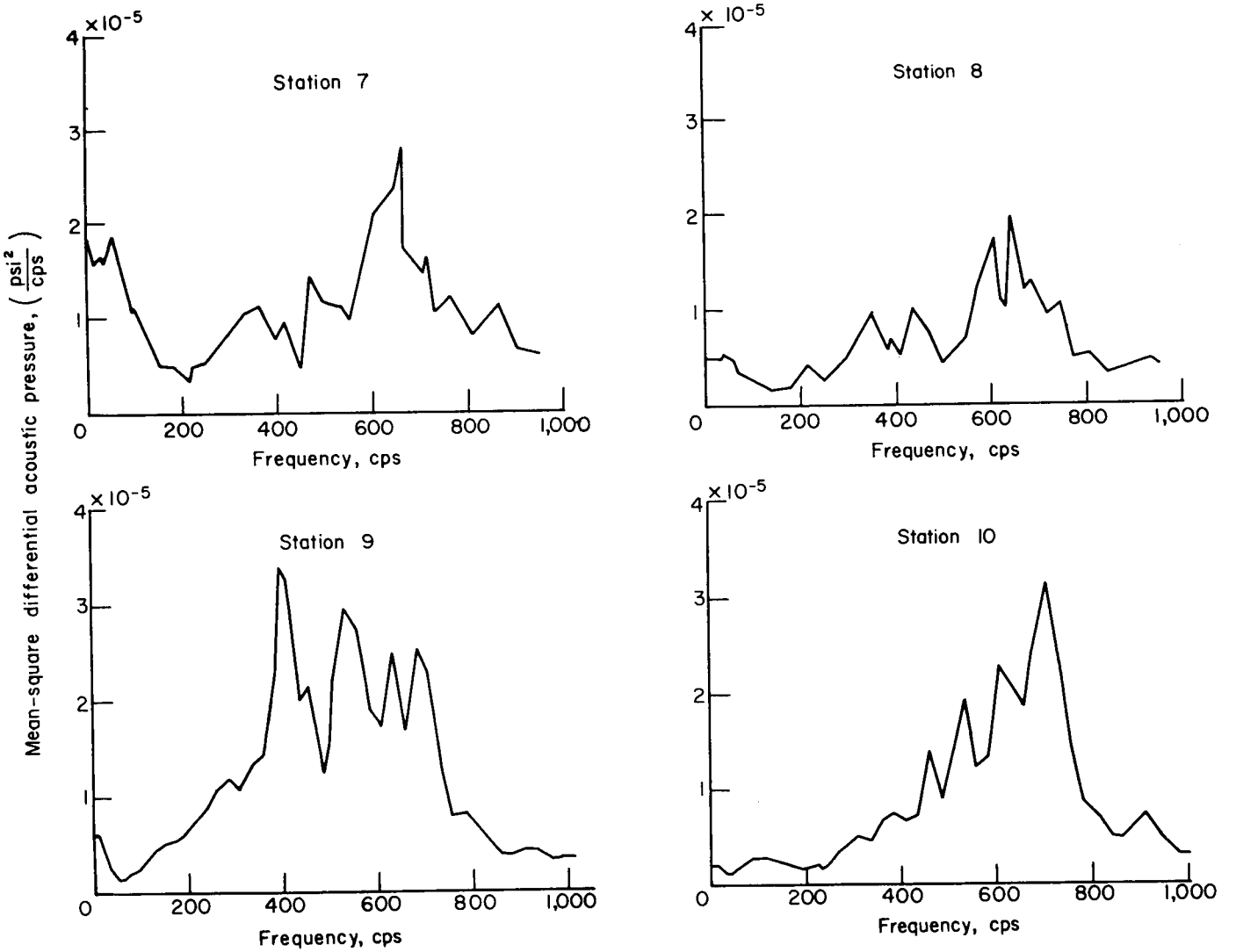

Figure 3.- Concluded.

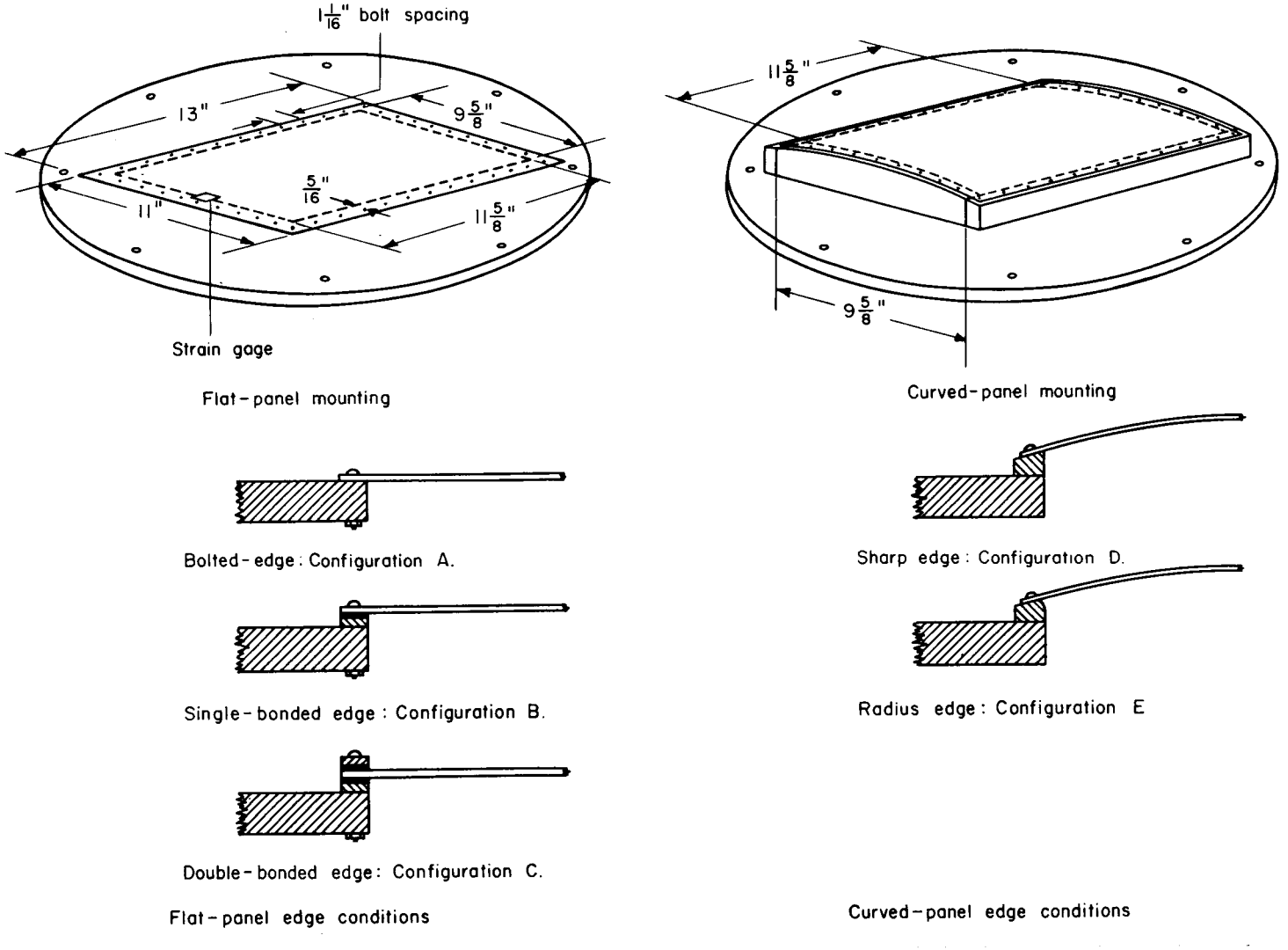

Figure 4.- Schematic diagrams of 2024-T3 aluminum-alloy test panels and mounting configurations.

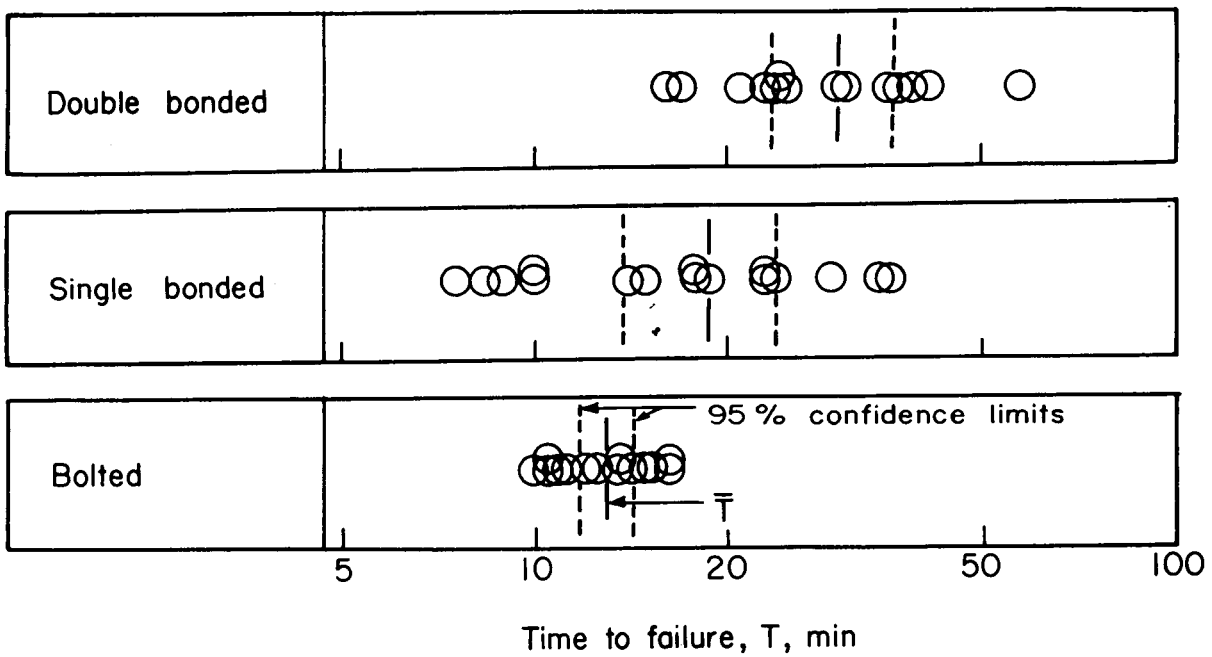

Figure 5.- Comparison of fatigue life of 0.032-inch flat panels with three edge conditions at air-jet station 1'. Overall random noise level 150 decibels (0 to 1,000 cps).

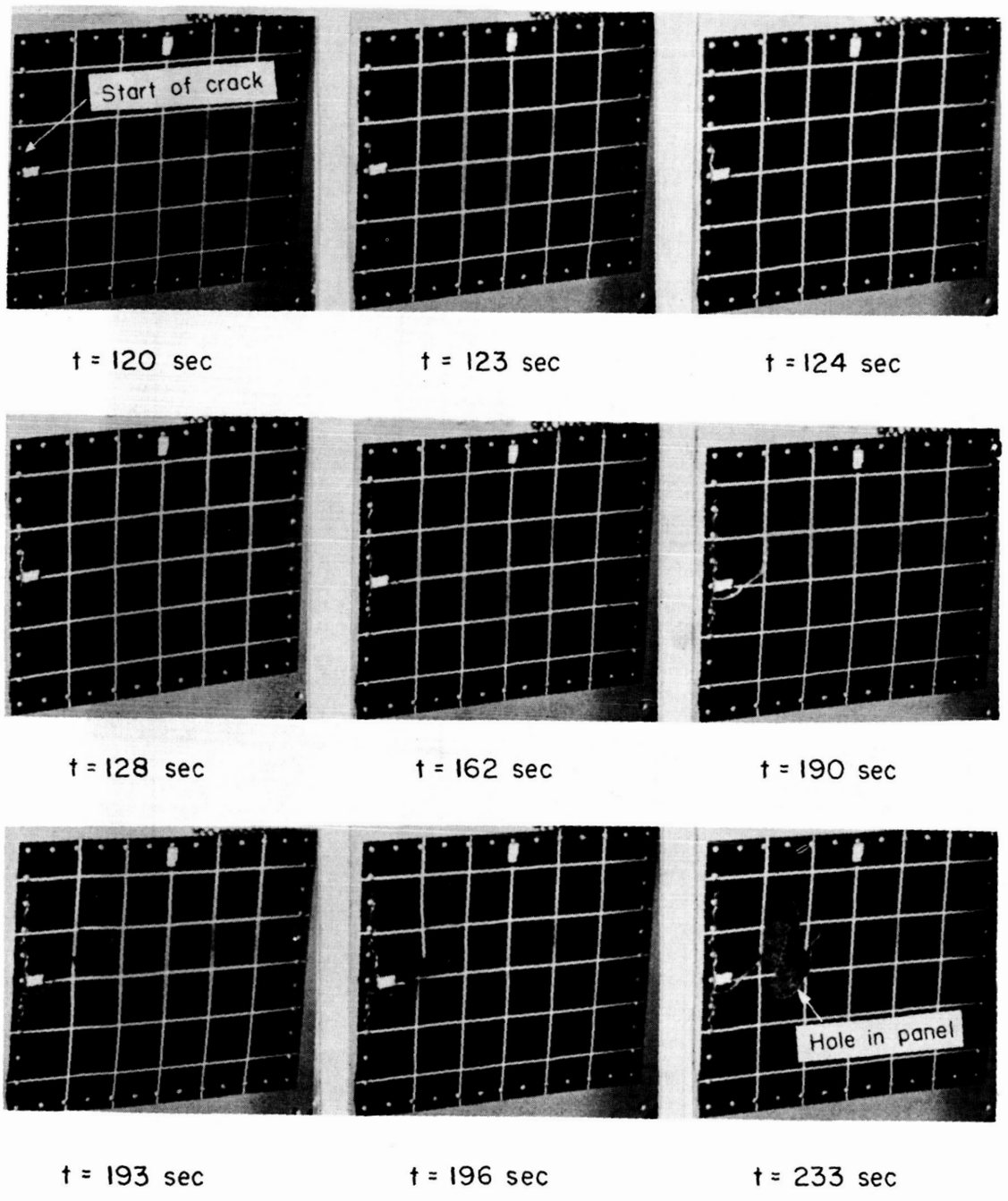

L-59-170

Figure 6.- Crack growth of 0.032-inch flat panel at a discrete noise level of 158 decibels.

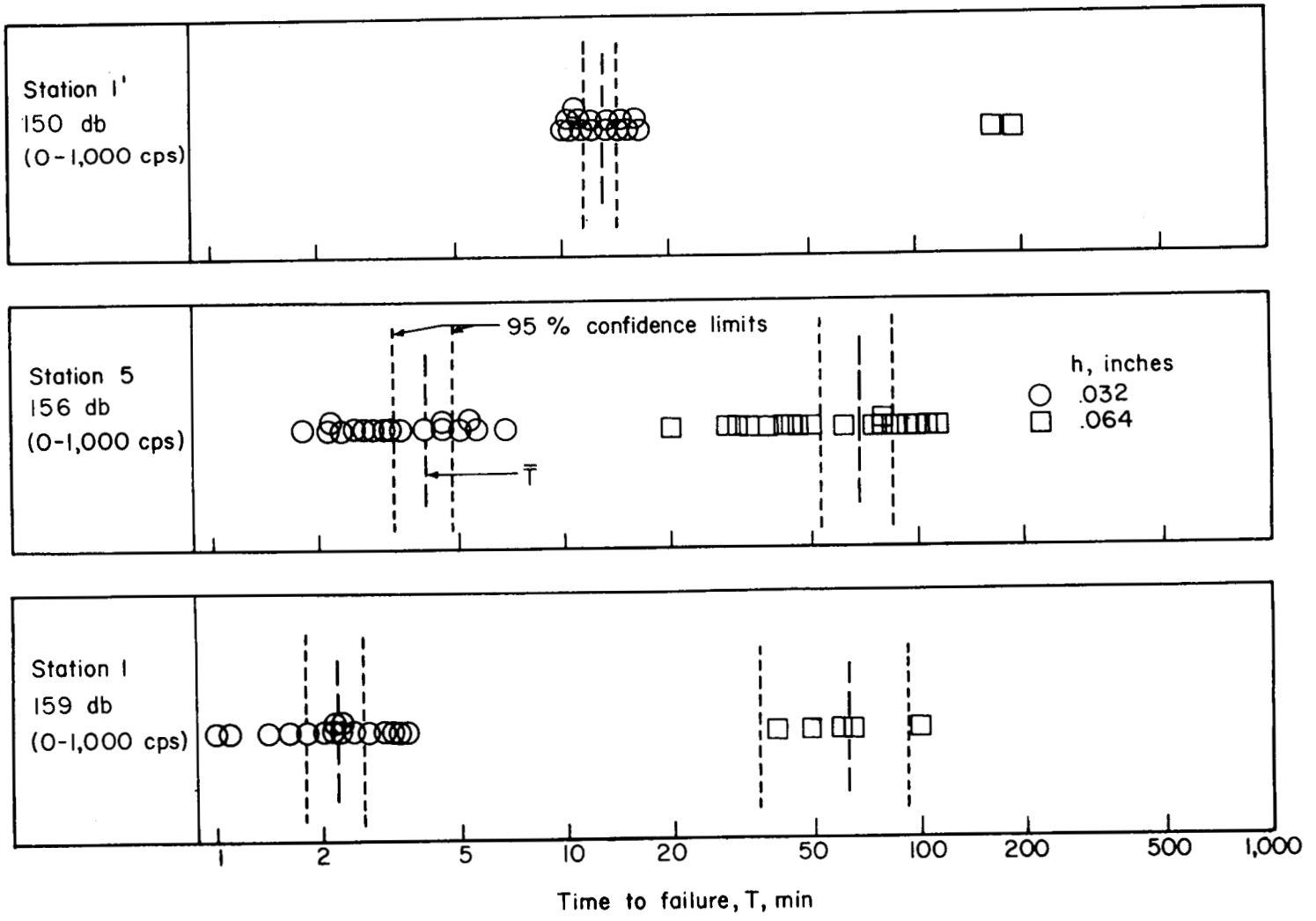

Figure 7.- Fatigue life of flat bolted 0.032- and 0.064-inch panels at three air-jet stations.

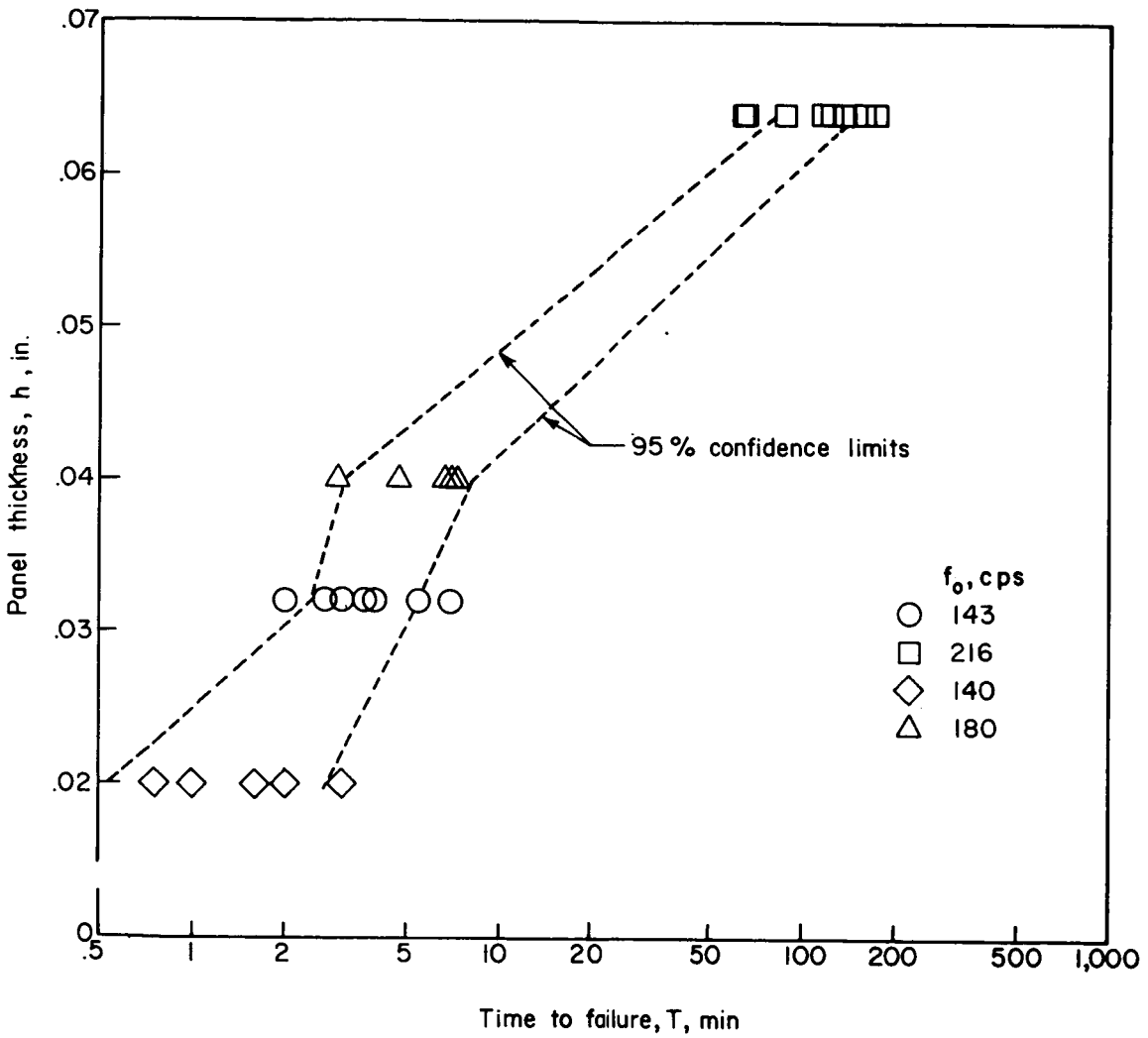

Figure 8.- Fatigue life as a function of panel thickness at a discrete noise level of 150 decibels.

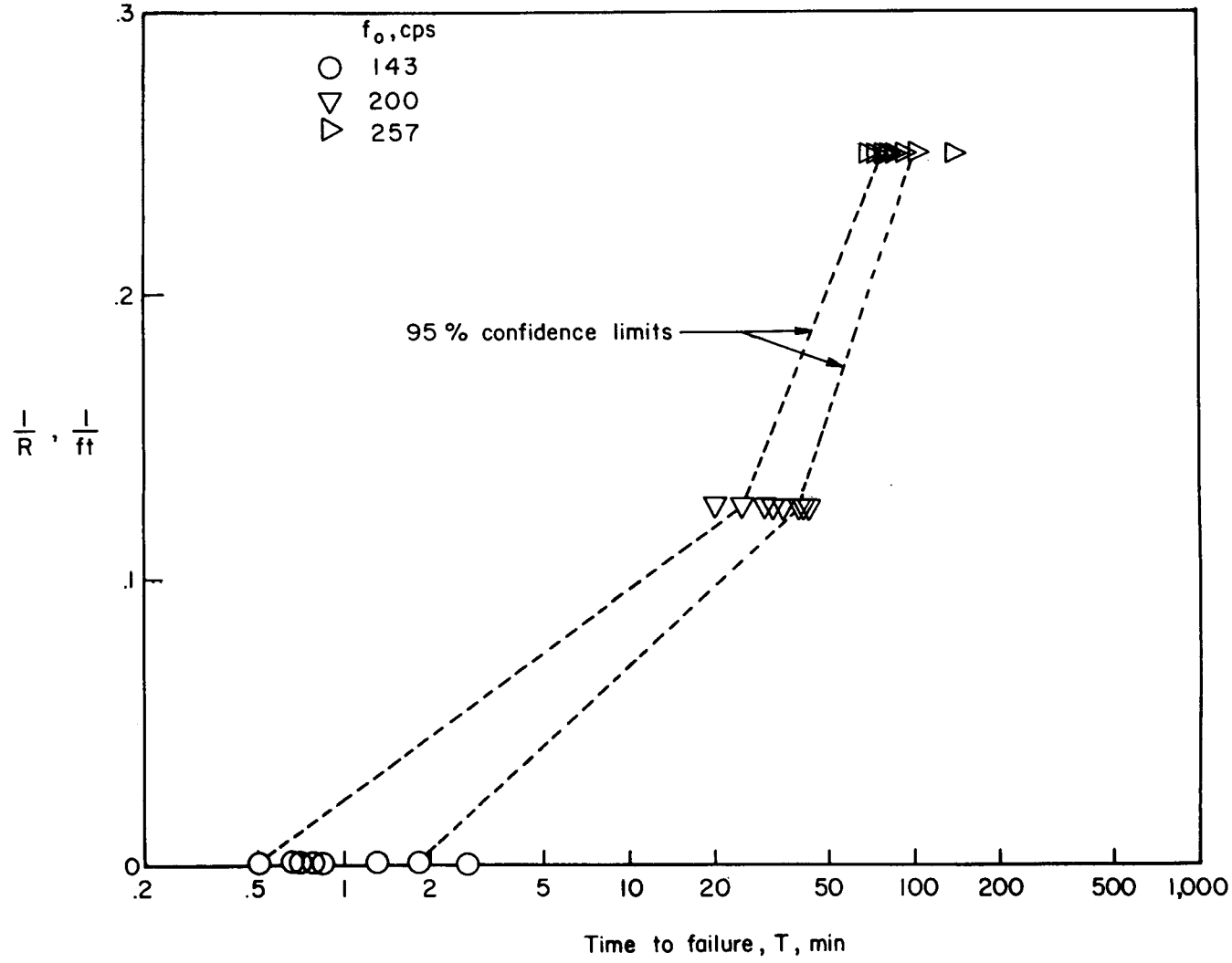

Figure 9.- Fatigue life of 0.032-inch panels as a function of panel curvature for three radii of curvature (R = ∞, 8 ft, and 4 ft). Configuration D. Discrete noise level, 154 decibels.

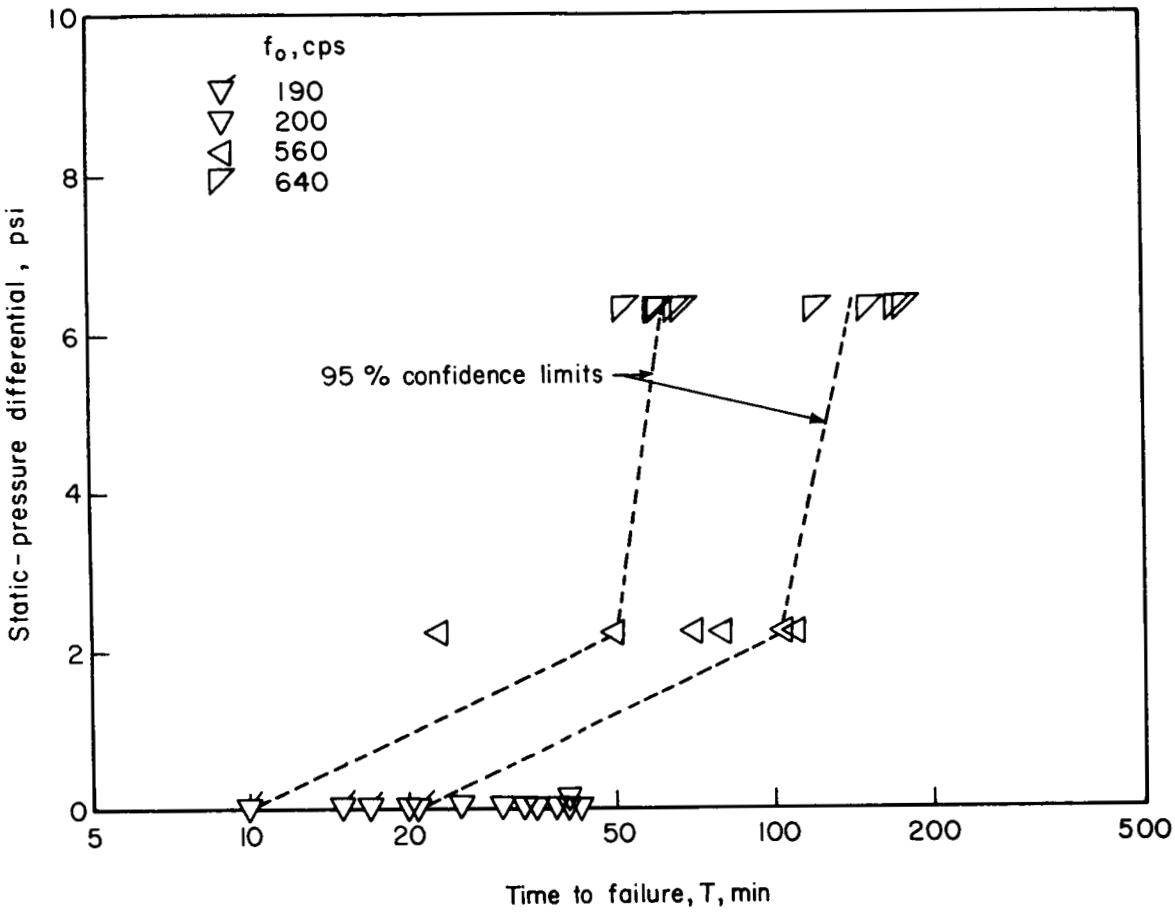

Figure 10. Fatigue life of 0.032-inch panels with an 8-foot radius of curvature as a function of static pressure on the concave surface at a discrete noise level of 154 decibels. Configuration D. (Flagged data points designate configuration E.)

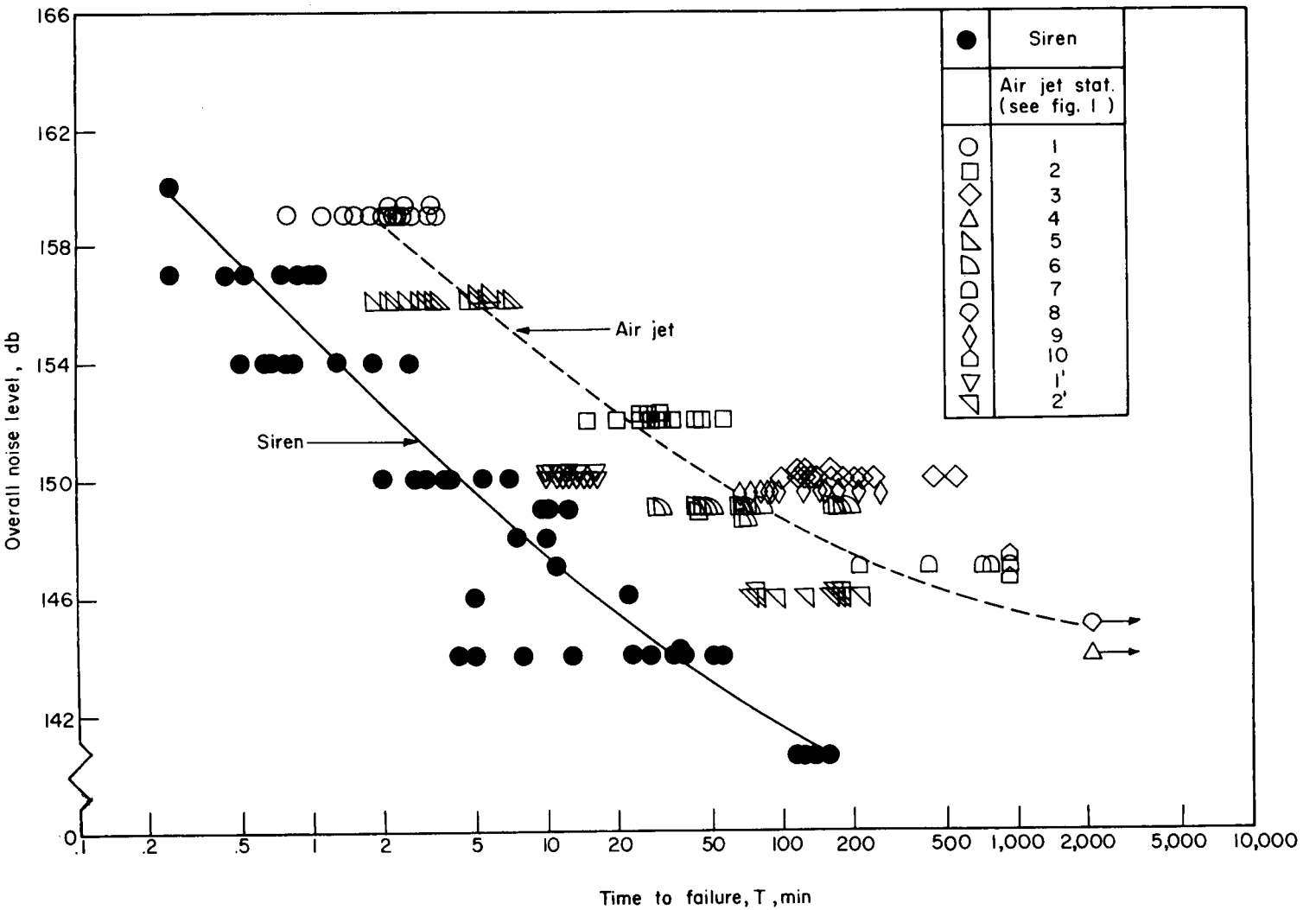

Figure 11.- Fatigue life of 0.032-inch panels as a function of overall noise level for both discrete and random loading.

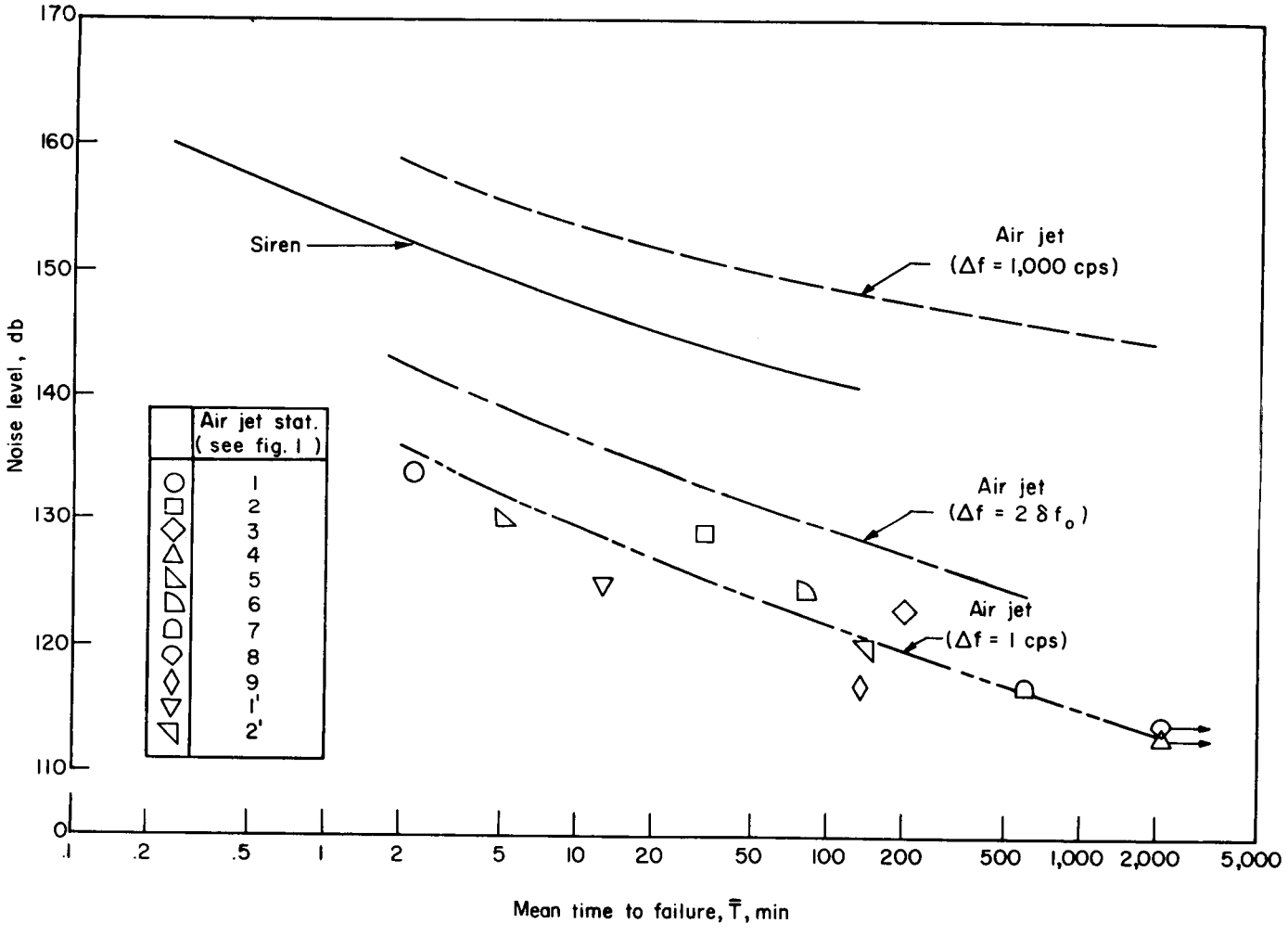

Figure 12.- Fatigue life of 0.032-inch panels as a function of siren and air-jet noise levels. Air-jet data are presented for band widths of 1 cps, 1,000 cps, and for a band width equal to the panel band width.

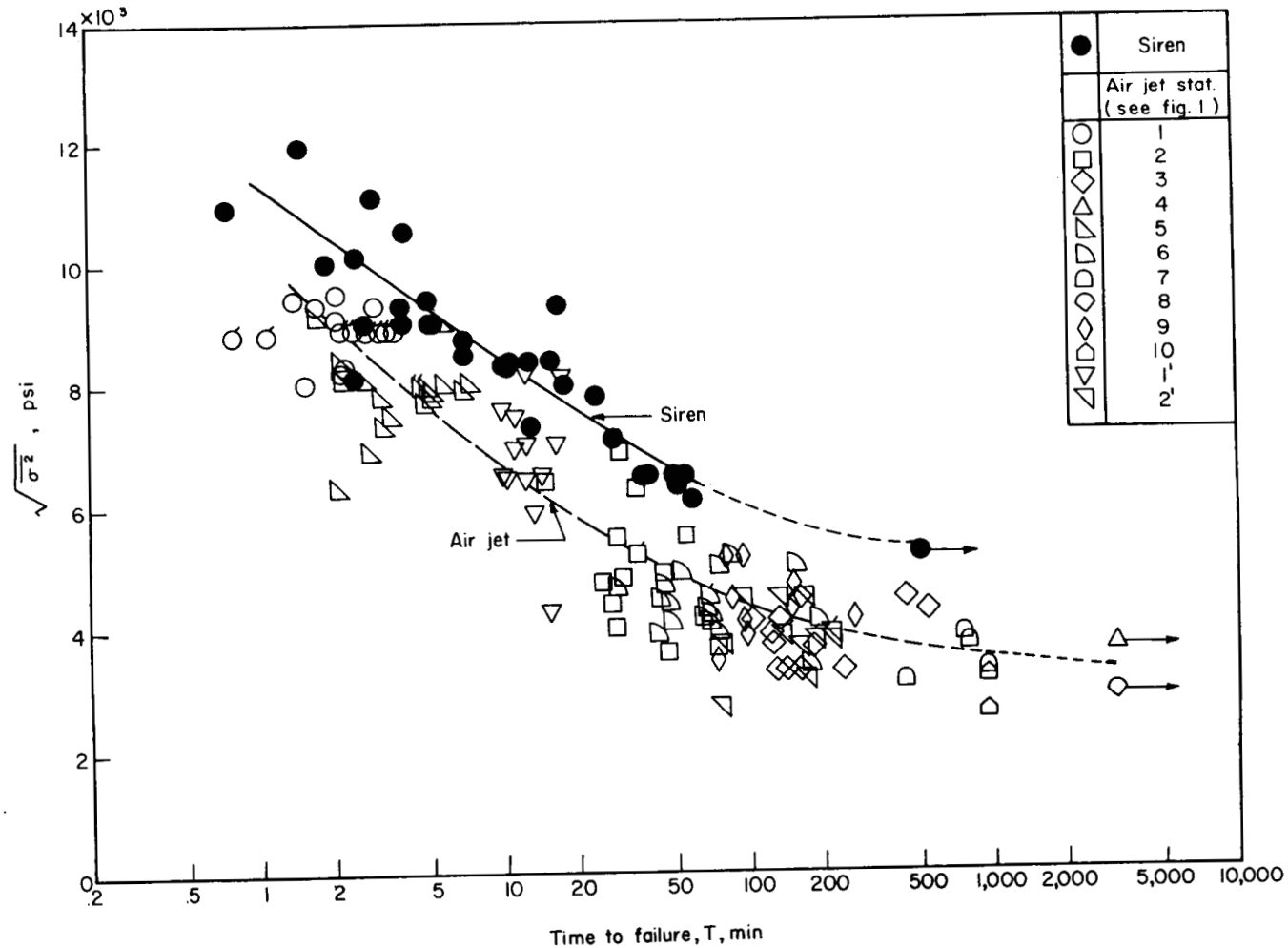

Figure 13.- Fatigue life of 0.032-inch panels as a function of root-mean-square stress for both discrete and random loadings. (Flagged symbols represent panels that failed before a stress reading could be obtained.)

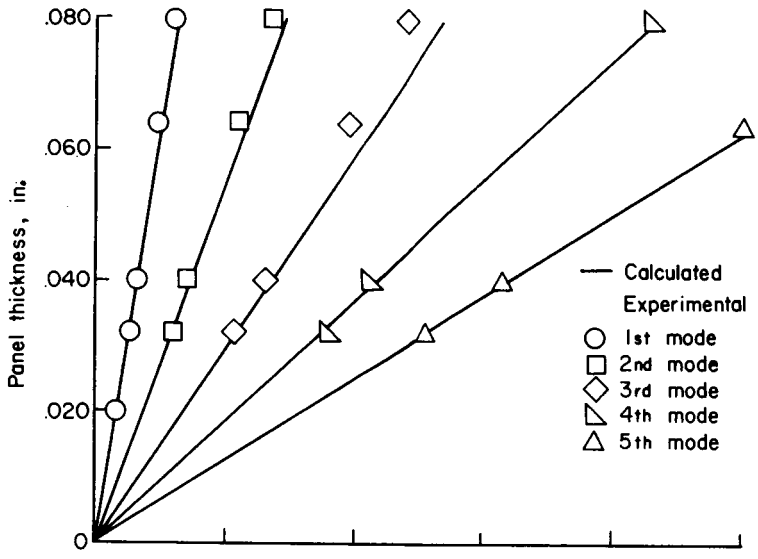

(a) Modes along Y-axis.

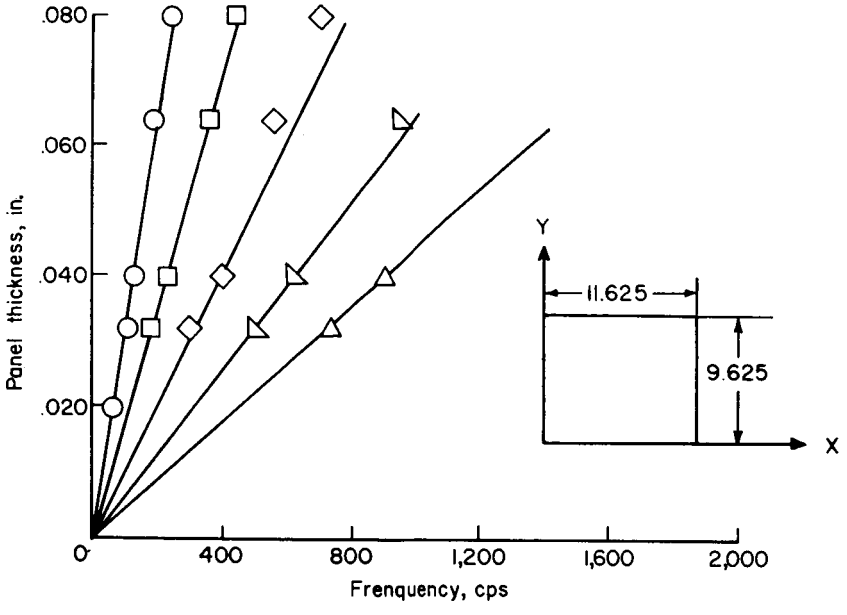

(b) Modes along X-axis.

Figure 14.- Comparison of calculated and experimental natural frequencies for flat panels of various thicknesses at small vibration amplitudes. (Experimental data apply to configuration A of figure 4; calculated results apply to the same unsupported lengths but with edges clamped.)

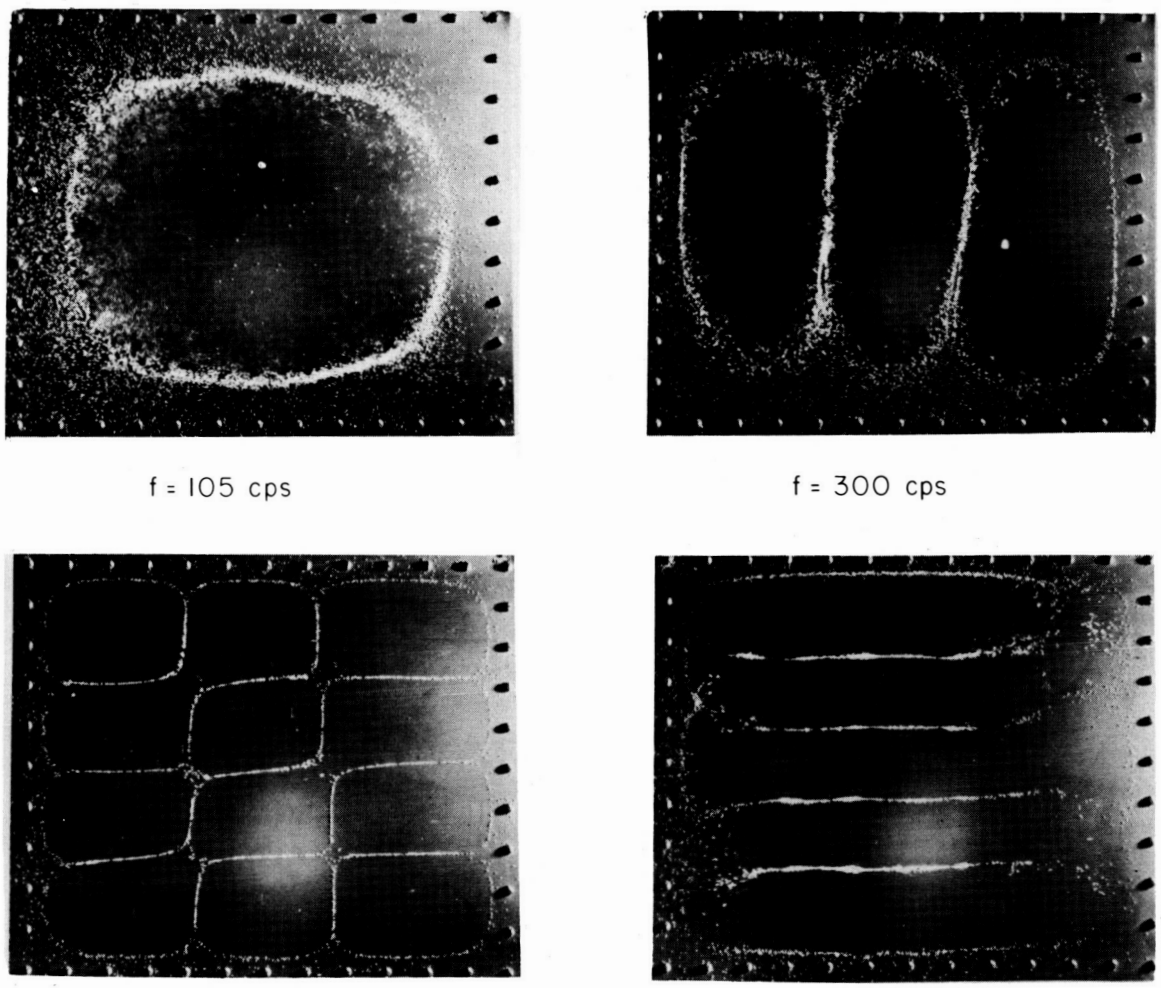

L-176

L-59-171

Figure 15.- Sample node lines of an 0.032-inch panel, configuration A of figure 4, excited by a loudspeaker at its natural frequencies.

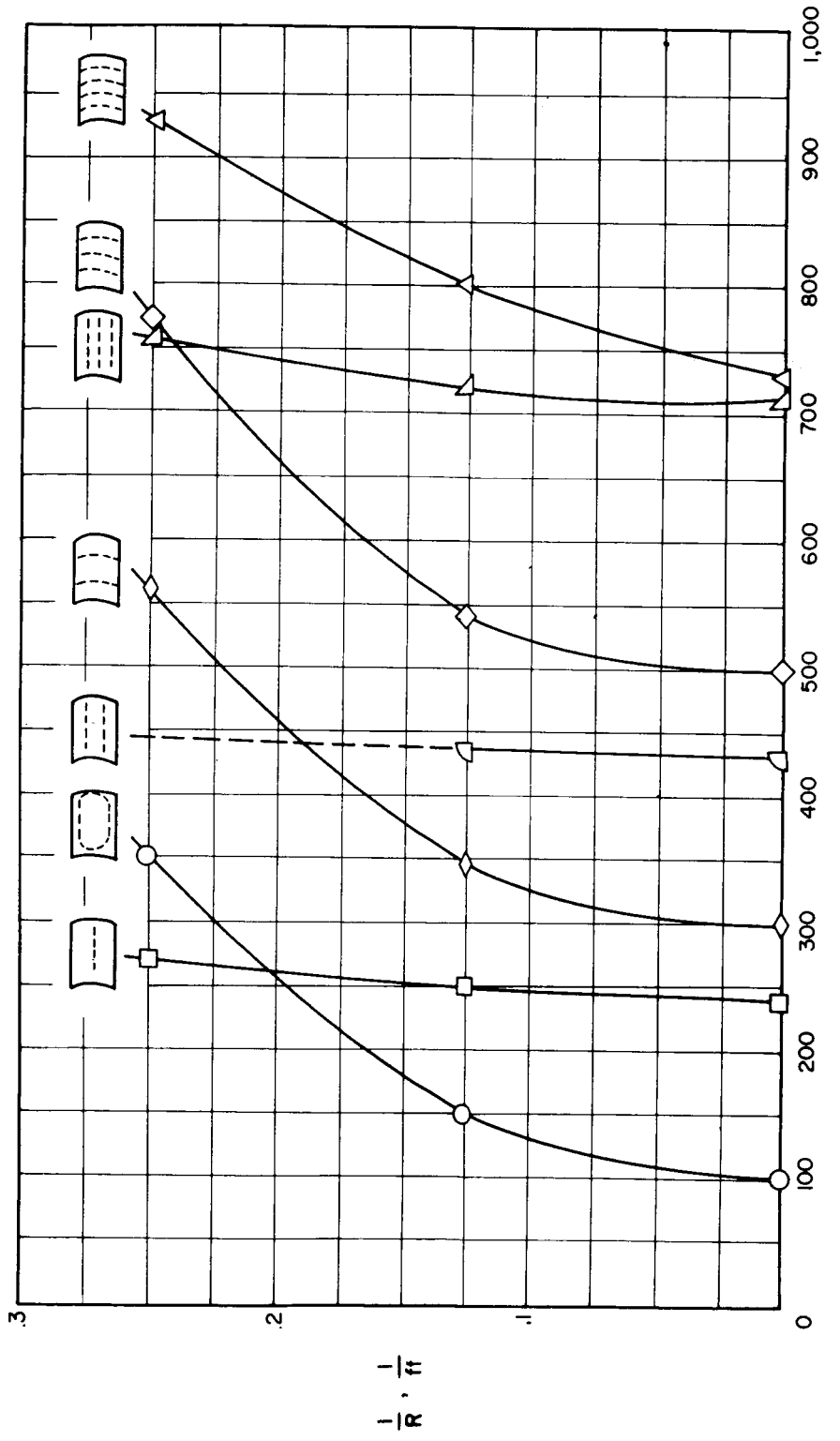

Figure 16.- Variations of natural frequencies with curvature for 0.032-inch panels with edge conditions as in configurations A and D of figure 4.